

Electronic Supplementary Information

Multi-site isomerization of synergistically regulated stimuli-responsive AIE materials toward multi-level decryption

Weiren Zhong,^{+[a,b]} Jianyu Zhang,^{+[c]} Yuting Lin,^[a] Shouji Li,^[a] Yalan Yang,^[a] Wen-Jin Wang,^[d] Chuanling Si,^{*[c]} Fritz E. Kühn,^[f] Zheng Zhao,^[d] Xu-Min Cai,^{*[a,b]} and Ben Zhong Tang ^{*[c,d]}

^[a]Jiangsu Co-Innovation Center of Efficient Processing and Utilization of Forest Resources, College of Chemical Engineering, Nanjing Forestry University, Nanjing 210037, China. ^[b]Guangdong Provincial Key Laboratory of Luminescence from Molecular Aggregates, Guangzhou 510640, China. ^[c]Department of Chemistry, Hong Kong Branch of Chinese National Engineering Research Center for Tissue Restoration and Reconstruction, The Hong Kong University of Science and Technology, Hongkong 999077, China. ^[d]School of Science and Engineering, Shenzhen Institute of Aggregate Science and Technology, The Chinese University of Hong Kong, Shenzhen (CUHK-Shenzhen), Shenzhen 518172, China. ^[e]State Key Laboratory of Biobased Fiber Manufacturing Technology, Tianjin Key Laboratory of Pulp and Paper, Tianjin University of Science and Technology, Tianjin 300457, China. ^[f]Molecular Catalysis, Department of Chemistry & Catalysis Research Center, School of Natural Sciences, Technische Universität München, München D-85747, Germany. ^[+]These authors contributed equally: Weiren Zhong and Jianyu Zhang.

*Corresponding author:

xumin.cai@njfu.edu.cn; sichli@tust.edu.cn; tangbenz@cuhk.edu.cn.

Contents

| | |
|--|------|
| Experimental Section | 1-3 |
| Materials and instrumentations | 1 |
| Synthetic procedures | 1 |
| | |
| Schemes, Figures, and Tables | 4-16 |
| Scheme S1. The synthesis routes of <i>p</i> -TPA-Br, <i>o</i> -Br-TPA, and <i>p</i> -Br-TPA. | 4 |
| Figure S1. ¹ H NMR spectrum of <i>p</i> -TPA-Br. | 4 |
| Figure S2. ¹³ C NMR spectrum of <i>p</i> -TPA-Br. | 5 |
| Figure S3. HRMS spectrum of <i>p</i> -TPA-Br. | 5 |
| Figure S4. ¹ H NMR spectrum of <i>o</i> -Br-TPA. | 6 |
| Figure S5. ¹³ C NMR spectrum of <i>o</i> -Br-TPA. | 6 |
| Figure S6. HRMS spectrum of <i>o</i> -Br-TPA. | 7 |
| Figure S7. ¹ H NMR spectrum of <i>p</i> -Br-TPA. | 7 |
| Figure S8. ¹³ C NMR spectrum of <i>p</i> -Br-TPA. | 8 |
| Figure S9. HRMS spectrum of <i>p</i> -Br-TPA. | 8 |
| Figure S10. Absorption spectra of <i>o</i> -TPA-Br, <i>p</i> -TPA-Br, <i>o</i> -Br-TPA, and <i>p</i> -Br-TPA in dilute ACN solution (20 μM). | 9 |
| Figure S11. PL spectra of <i>o</i> -Br-TPA in ACN solution with different concentrations. | 9 |
| Figure S12. (a) PL spectra of <i>o</i> -Br-TPA in EtOH/glycerol mixtures with different fractions of glycerol. (b) The plots of the enol and keto emission intensity at the maximum versus the composition of the glycerol mixture of <i>o</i> -Br-TPA. (c) The plot of keto/enol emission intensity at the maximum versus the composition of the glycerol mixture of <i>o</i> -Br-TPA. | 10 |
| Figure S13. Fluorescence photographs of <i>o</i> -Br-TPA (in ACN), and <i>p</i> -Br-TPA (in THF) at RT and 77 K, respectively. | 10 |
| Figure S14. Absorption spectra of (a) <i>o</i> -TPA-Br, (b) <i>p</i> -TPA-Br, (c) <i>o</i> -Br-TPA, and (d) <i>p</i> -Br-TPA in solvents of varying polarity. | 11 |
| Figure S15. The PL spectra of (a) <i>o</i> -TPA-Br, (b) <i>p</i> -TPA-Br, (c) <i>o</i> -Br-TPA, and (d) <i>p</i> -Br-TPA in solvents of varying polarity. | 12 |
| Figure S16. The molecular structures of isomers that regulate excited-state processes. | 13 |
| Table S1. Crystallographic data for <i>o</i> -Br-TPA and <i>p</i> -Br-TPA. | 14 |
| Figure S17. The photographs of (a) <i>o</i> -TPA-Br and (b) <i>o</i> -Br-TPA before and after grinding tanken under 365 nm lamp irradiation. | 15 |
| Figure S18. The chemical conformations, dimers, and packings of (a) <i>o</i> -TPA-Br and (b) <i>o</i> -Br-TPA. | 15 |
| Figure S19. Fluorescence photographs of (a) <i>o</i> -TPA-Br and (b) <i>o</i> -Br-TPA as solid (pristine, sample fumed with TFA, sample fumed with TEA). | 16 |
| Figure S20. Absorption spectra of (a) <i>o</i> -TPA-Br, (b) <i>p</i> -TPA-Br, and (c) <i>o</i> -Br-TPA in pure | |

| | |
|---|----|
| ACN by adding different equivalents of TFA. | 16 |
| Figure S21. ¹ H NMR spectra of (a) <i>o</i> -TPA-Br and (b) <i>o</i> -Br-TPA in CDCl ₃ before and after TFA fuming in 6.0–14.0 ppm region. | 17 |
| Figure S22. Fluorescence photographs of the ground <i>p</i> -TPA-Br before and after TFA/TEA treatments. | 17 |
| References | 17 |

Experimental Section

Materials and instrumentations

Unless specific requirements, all the organic solvents are purchased and used without additional purifications. *o*-TPA-Br is synthesized according to a previous report [1]. 4-(Diphenylamino) phenylboronic acid (Aladdin, 98%), 5-bromosalicylaldehyde (Aladdin, 98%), 4-bromoaniline (Aladdin, 99%), 2-bromoaniline (Aladdin, 98%), tetrakis (triphenylphosphine) palladium (Energy Chemical, 99%), trifluoroacetic acid (TFA) (Energy Chemical, 99%), and triethylamine (TEA) (Sinopharm Chemical Reagent Co., Ltd., 99.0%) are purchased and used directly without further purification. Nuclear magnetic resonance (NMR) spectra are obtained using a Bruker AVANCE III HD spectrometer (600 MHz for ¹H and 150 MHz for ¹³C) in a solution of CDCl₃. High-resolution mass spectrometry (HRMS) spectra are acquired using a Q Exactive (Thermo Scientific, Germany) mass spectrometer operating with an ESI mode. Ultraviolet-visible (UV–Vis) absorption spectra are measured on a Shimadzu UV-2450 spectrometer. Photoluminescence (PL) spectra are performed on a Fluoromax-4 spectrofluorometer. UV–Vis diffuse reflectance (UV-DRS) spectra are acquired utilizing a PE Lambda 950 UV–Vis–NIR spectrometer. Powder X-ray diffraction (PXRD) experiments are conducted using a Rigaku Ultima IV diffractometer with Cu K α radiation. Single-crystal data of *o*-TPA-Br (CCDC = 2190006) is from a previous report [1]. Single-crystal data of *o*-Br-TPA (CCDC = 2293108) is selected and mounted on CCD area detector using Mo K α radiation ($\lambda = 0.71073 \text{ \AA}$). Single-crystal data of *p*-Br-TPA (CCDC = 2252820) is selected and mounted on an Xcalibur, Eos, Gemini diffractometer using Cu K α radiation ($\lambda = 1.54184 \text{ \AA}$).

Synthetic procedures

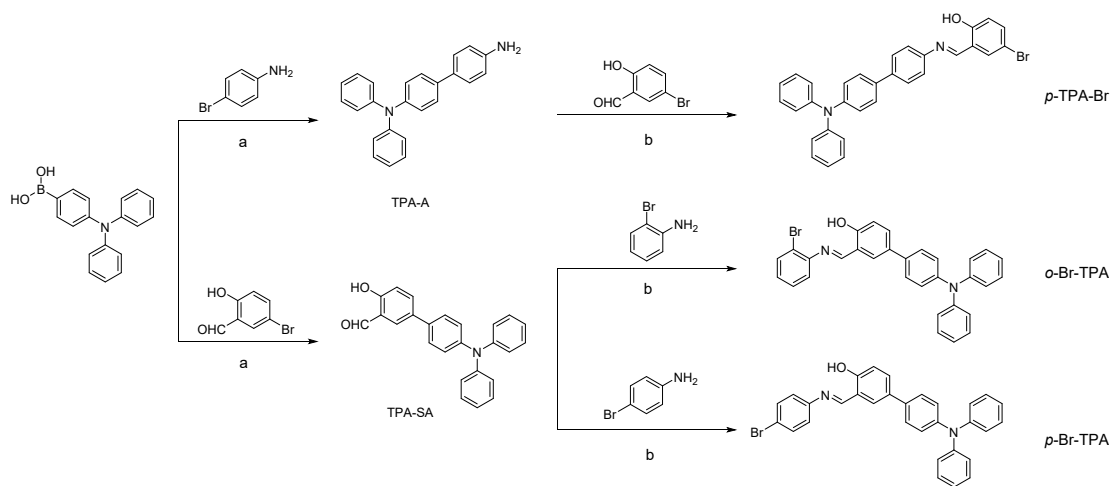
***p*-TPA-Br:** 4-(Diphenylamino) phenylboronic acid (300 mg, 1.04 mmol), 4-bromoaniline (214 mg, 1.25 mmol), tetrakis (triphenylphosphine) palladium (48 mg, 0.04 mmol), and 1 mL of saturated K₂CO₃ are added rapidly to a 3 mL solution of toluene. These feeding processes are conducted under N₂ atmosphere. After stirring the reaction mixture at 115 °C for 6 h, it is extracted with DCM/H₂O and then purified by silica gel column chromatography using eluents of petroleum ether/ethyl acetate (volume ratio: 20/1). Then, the intermediate of A-TPA is

obtained with a yield of 60%. A-TPA (100 mg, 0.30 mmol) is slowly added to a vigorously stirred solution of 5-bromosalicylaldehyde (72 mg, 0.36 mmol) in 20 mL of EtOH. The reaction mixture is refluxed for 3 h and cooled to room temperature afterward. Yield: 80%. ^1H NMR (600 MHz, CDCl_3) δ 13.37 (s, 1H), 8.61 (s, 1H), 7.64 (d, $J = 8.4$ Hz, 2H), 7.52 (d, 1H), 7.50 (d, $J = 8.6$ Hz, 2H), 7.45 (dd, $J = 8.8, 2.4$ Hz, 1H), 7.35 (d, $J = 8.4$ Hz, 2H), 7.28 (t, $J = 7.9$ Hz, 4H), 7.15 (d, $J = 8.4$ Hz, 6H), 7.06 (t, $J = 7.3$ Hz, 2H), 6.94 (d, $J = 8.8$ Hz, 1H). ^{13}C NMR (150 MHz, CDCl_3) δ 160.55, 160.32, 147.69, 140.02, 135.77, 134.30, 129.46, 127.69, 124.70, 123.84, 123.25, 121.80, 120.83, 119.40, 110.65. HRMS (ESI, m/z): $[\text{M}+\text{H}]^+$ calcd for $\text{C}_{31}\text{H}_{24}\text{BrN}_2\text{O}$: 519.1067; found: 519.1053.

***o*-Br-TPA:** 4-(Diphenylamino) phenylboronic acid (300 mg, 1.04 mmol), 5-bromosalicylaldehyde (250 mg, 1.25 mmol), tetrakis (triphenylphosphine) palladium (48 mg, 0.04 mmol), and 1 mL of saturated K_2CO_3 are added rapidly to a 3 mL solution of toluene. The subsequent reaction conditions and post-treatment methods are consistent with ATPA-*p*-SAB. The intermediate of TPA-SA is obtained with a yield of 60%. TPA-SA (100 mg, 0.27 mmol) is slowly added to a vigorously stirred solution of 2-bromoaniline (56 mg, 0.32 mmol) in 20 mL of EtOH. The reaction mixture is refluxed for 3 h and cooled to room temperature afterward. Yield: 80%. ^1H NMR (600 MHz, CDCl_3) δ 13.13 (s, 1H), 8.67 (s, 1H), 7.70 (d, $J = 7.9$ Hz, 1H), 7.66 – 7.60 (m, 2H), 7.45 (d, $J = 8.1$ Hz, 2H), 7.39 (t, $J = 7.6$ Hz, 1H), 7.32 – 7.26 (m, 4H), 7.22 – 7.08 (m, 9H), 7.05 (t, $J = 7.2$ Hz, 3H). ^{13}C NMR (150 MHz, CDCl_3) δ 163.32, 160.56, 147.80, 147.05, 146.84, 134.17, 133.46, 132.23, 130.41, 128.64, 127.33, 124.47, 124.26, 123.05, 120.16, 119.23, 118.07. HRMS (ESI, m/z): $[\text{M}+\text{H}]^+$ calcd for $\text{C}_{31}\text{H}_{24}\text{BrN}_2\text{O}$: 519.1067; found: 519.1046.

***p*-Br-TPA:** TPA-SA (100 mg, 0.27 mmol) is slowly added to a vigorously stirred solution of 4-bromoaniline (56 mg, 0.32 mmol) in 20 mL of EtOH. The reaction mixture is refluxed for 3 h and cooled to room temperature afterward. Yield: 80%. ^1H NMR (600 MHz, CDCl_3) δ 12.97 (s, 1H), 8.66 (s, 1H), 7.62 (dd, $J = 8.6, 2.3$ Hz, 1H), 7.59 (d, $J = 2.3$ Hz, 1H), 7.57–7.53 (m, 2H), 7.46–7.42 (m, 2H), 7.38–7.27 (m, 4H), 7.19–7.17 (m, 2H), 7.16–7.12 (m, 6H), 7.09 (d, $J = 8.6$ Hz, 1H), 7.04 (t, $J = 7.4$ Hz, 2H). ^{13}C NMR (150 MHz, CDCl_3) δ 163.20, 160.42, 147.84, 147.67, 147.12, 134.18, 132.69, 132.24, 132.02, 129.44, 127.34, 124.52, 124.27, 123.09,

122.98, 120.63, 119.27. HRMS (ESI, m/z): $[M+H]^+$ calcd for $C_{31}H_{24}BrN_2O$: 519.1067; found: 519.1055.



Scheme S1. The synthesis routes of *p*-TPA-Br, *o*-Br-TPA, and *p*-Br-TPA. (a) Toluene, Pd(PPh₃)₄, K₂CO₃, 6 h. (b) EtOH, 3 h.

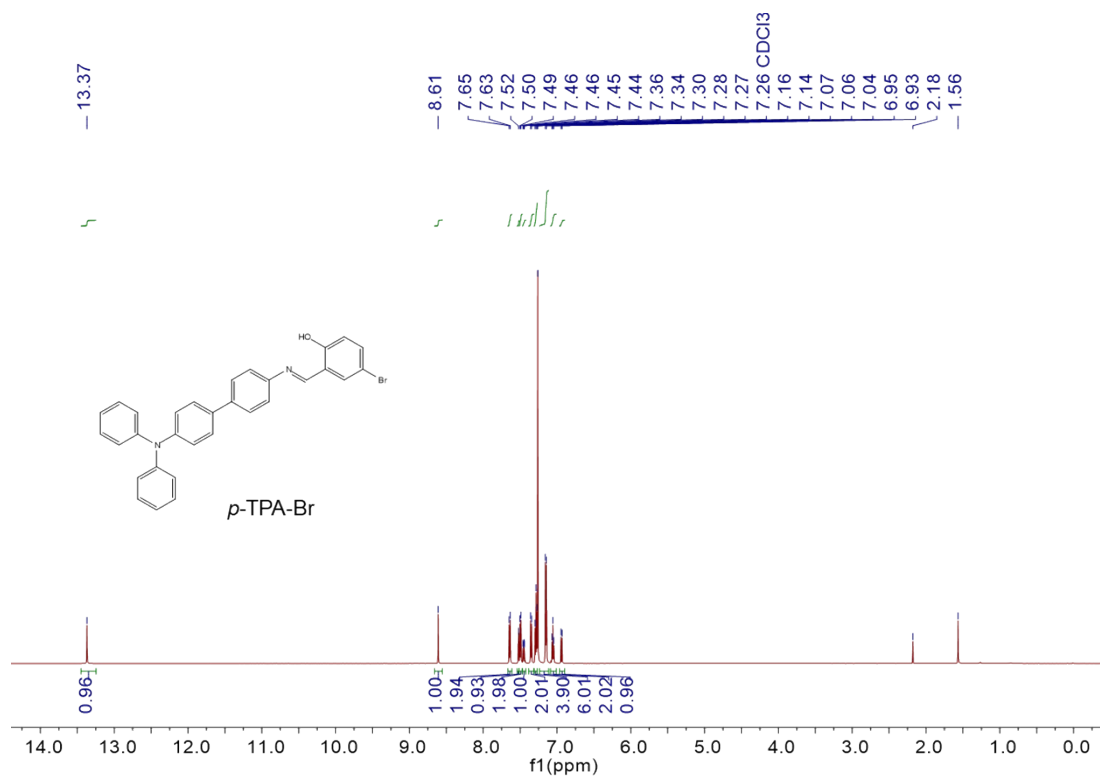


Figure S1. ¹H NMR spectrum of *p*-TPA-Br.

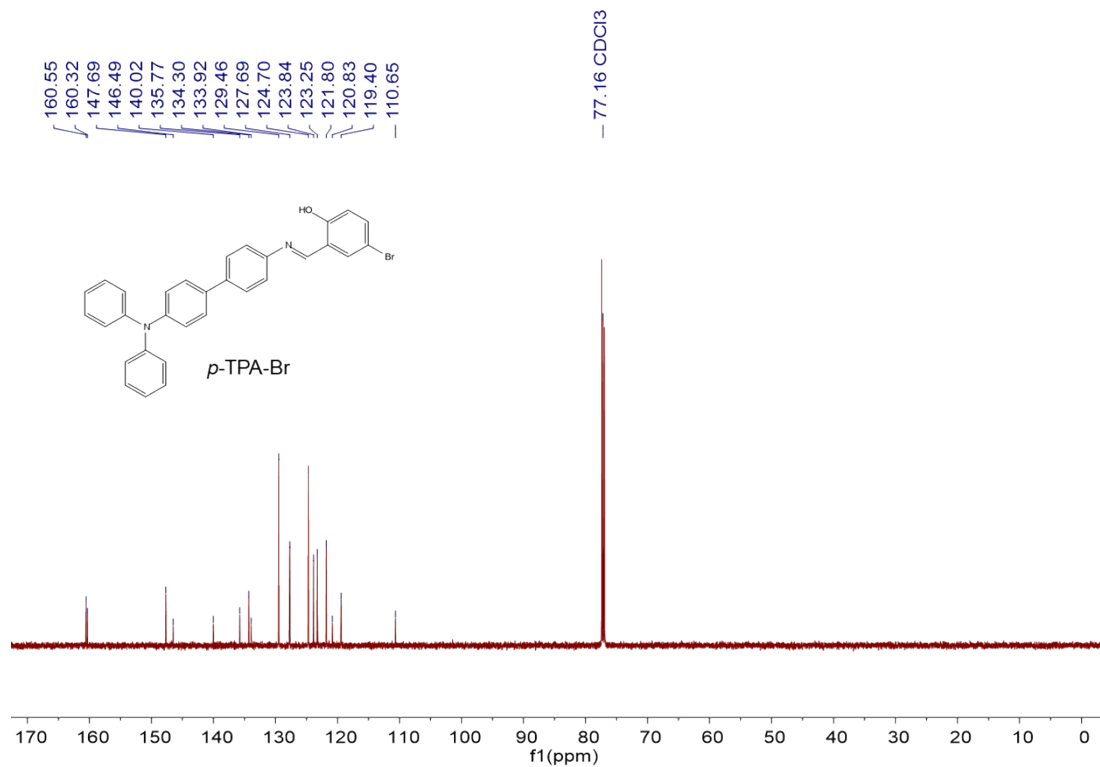


Figure S2. ^{13}C NMR spectrum of *p*-TPA-Br.

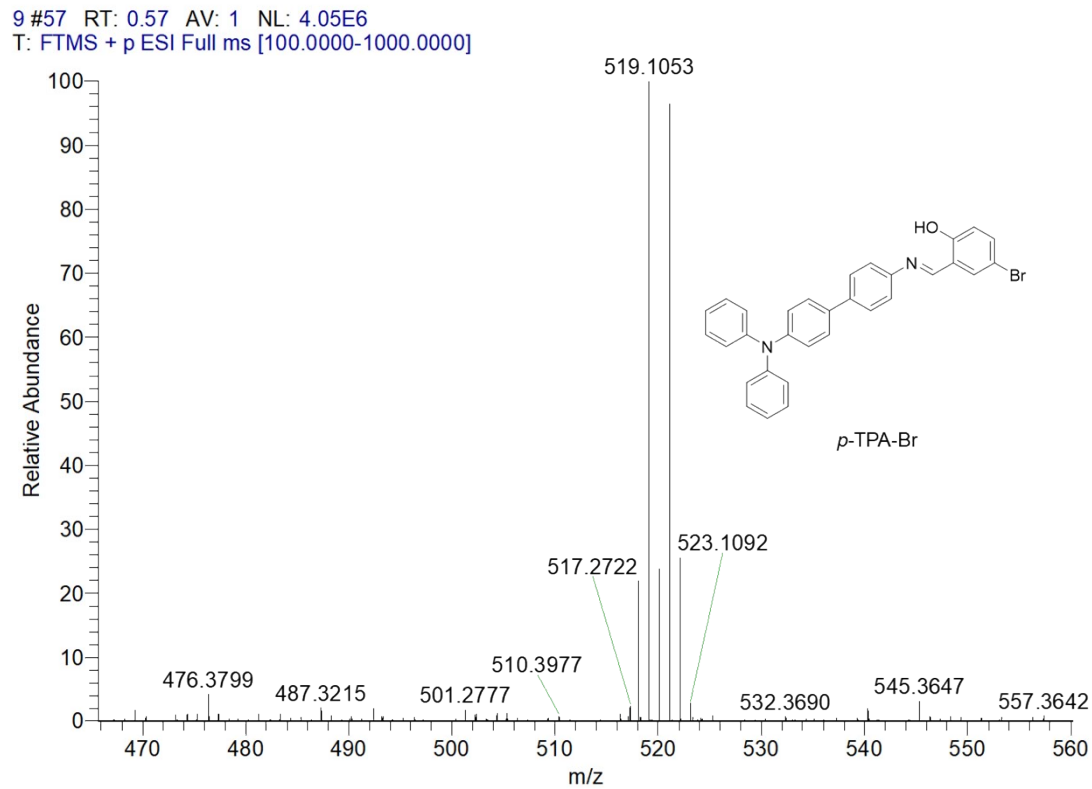


Figure S3. HRMS spectrum of *p*-TPA-Br.

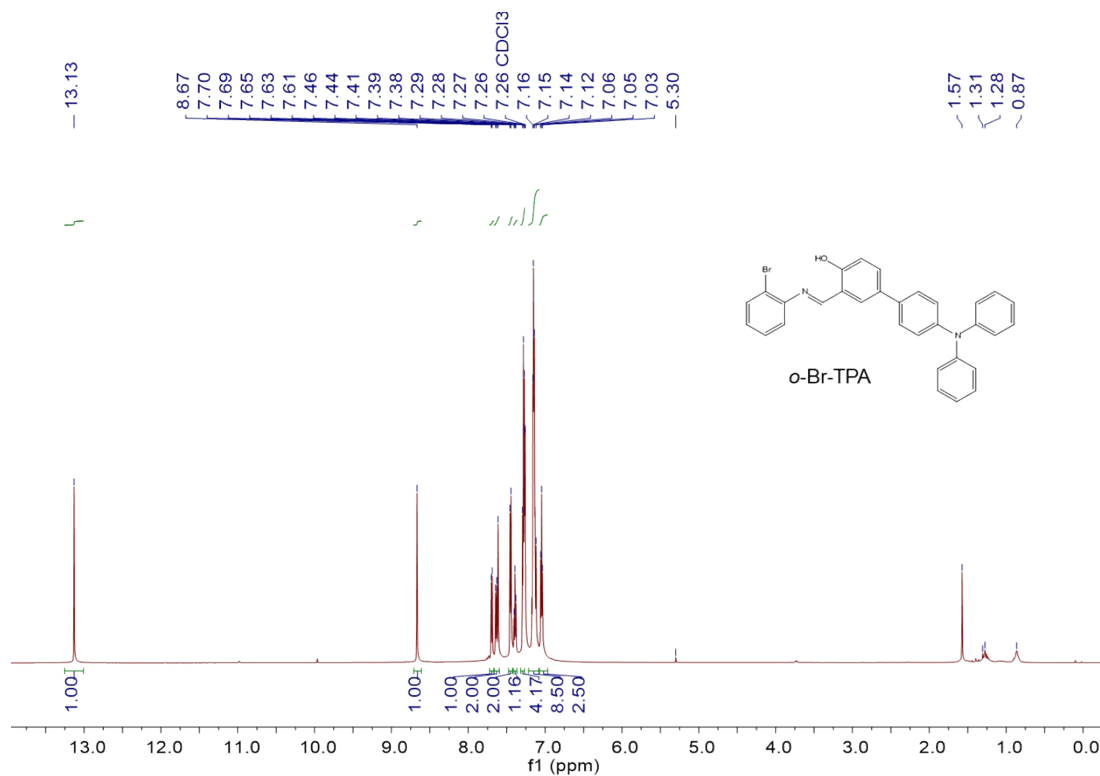


Figure S4. ¹H NMR spectrum of *o*-Br-TPA.

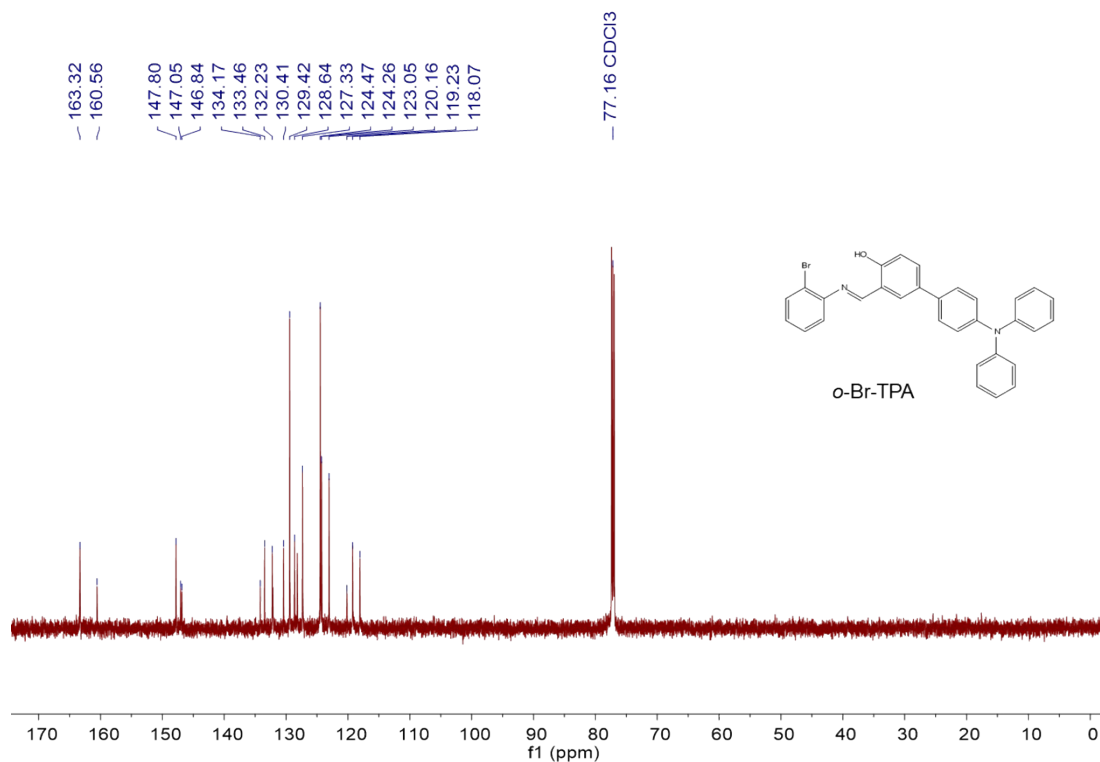


Figure S5. ¹³C NMR spectrum of *o*-Br-TPA.

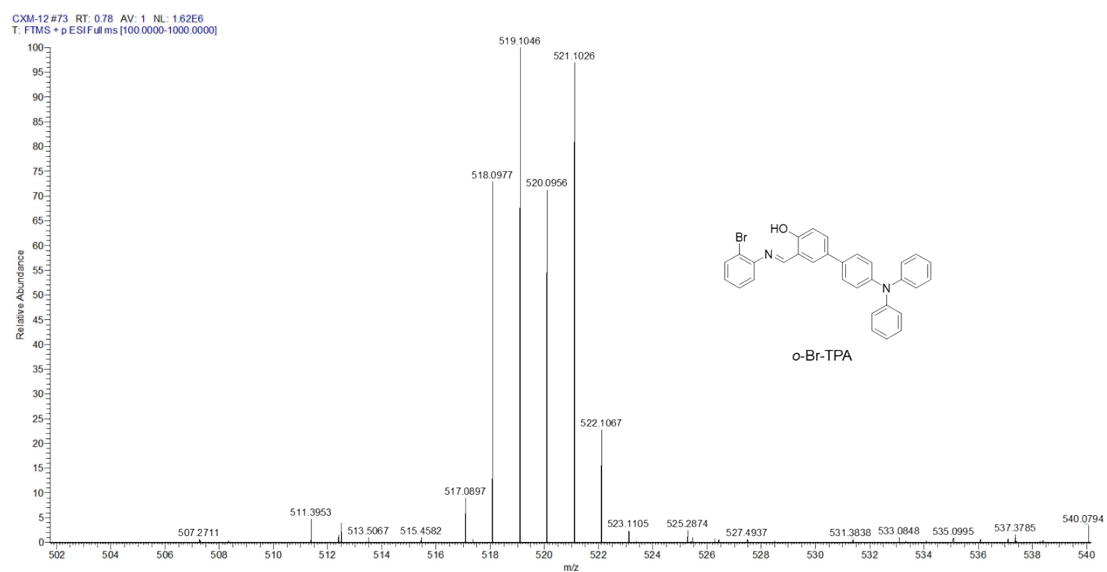


Figure S6. HRMS spectrum of *o*-Br-TPA.

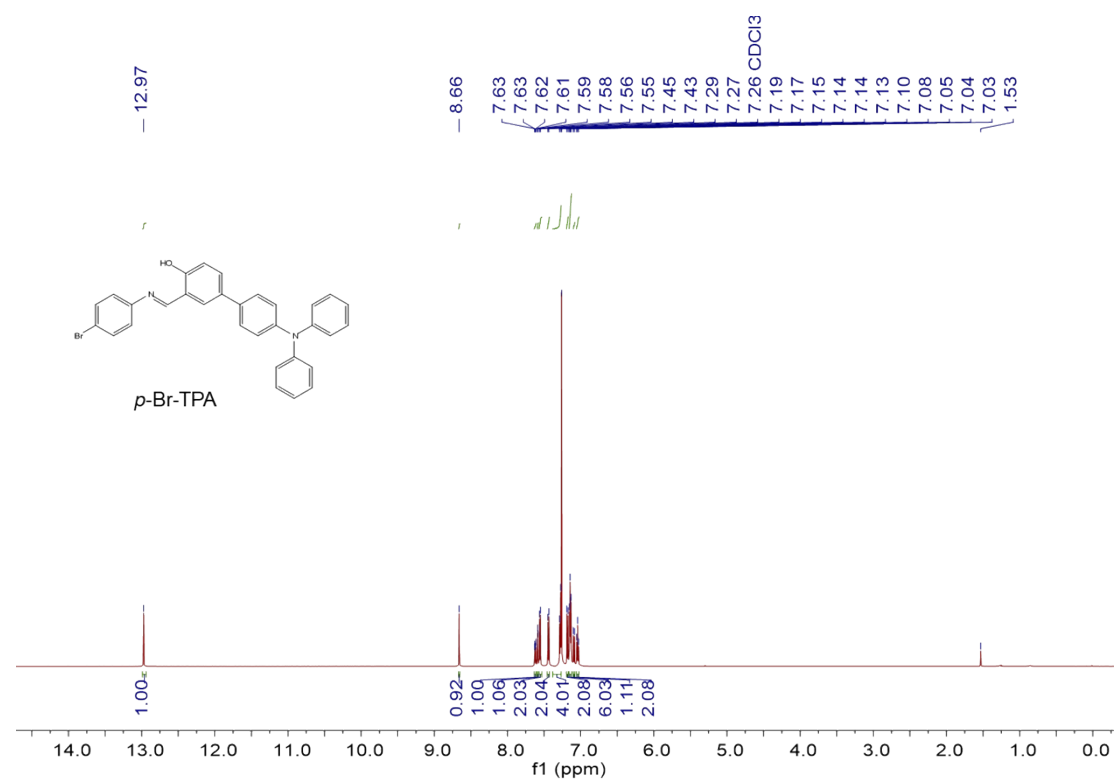


Figure S7. ¹H NMR spectrum of *p*-Br-TPA.

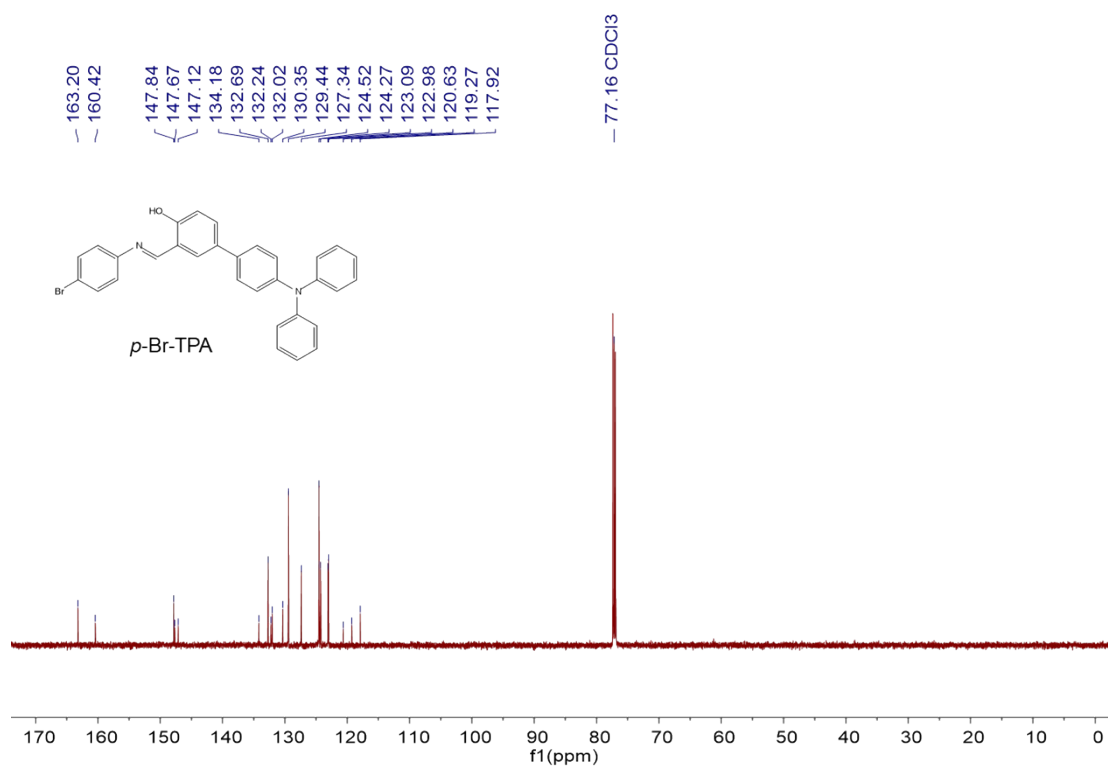


Figure S8. ¹³C NMR spectrum of *p*-Br-TPA.

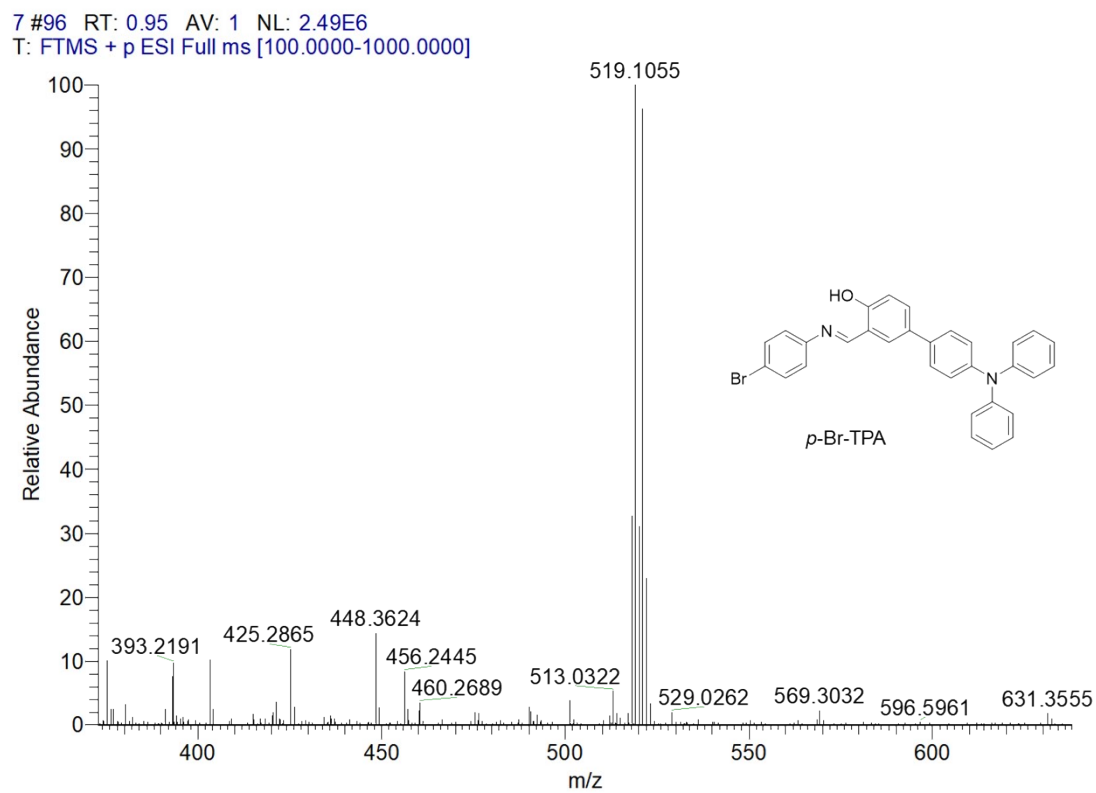


Figure S9. HRMS spectrum of *p*-Br-TPA.

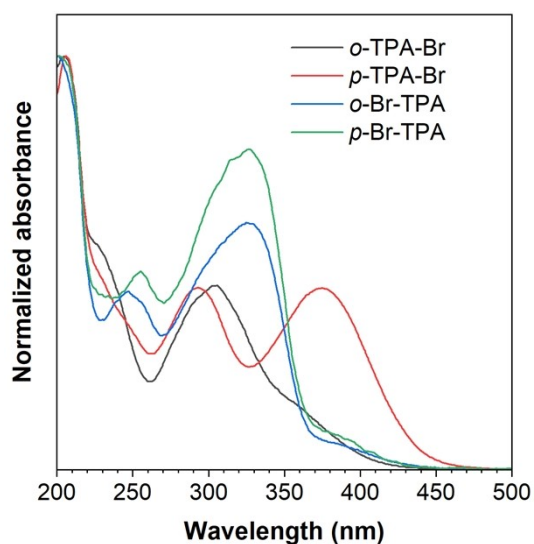


Figure S10. Absorption spectra of *o*-TPA-Br, *p*-TPA-Br, *o*-Br-TPA, and *p*-Br-TPA in dilute ACN solution (20 μ M).

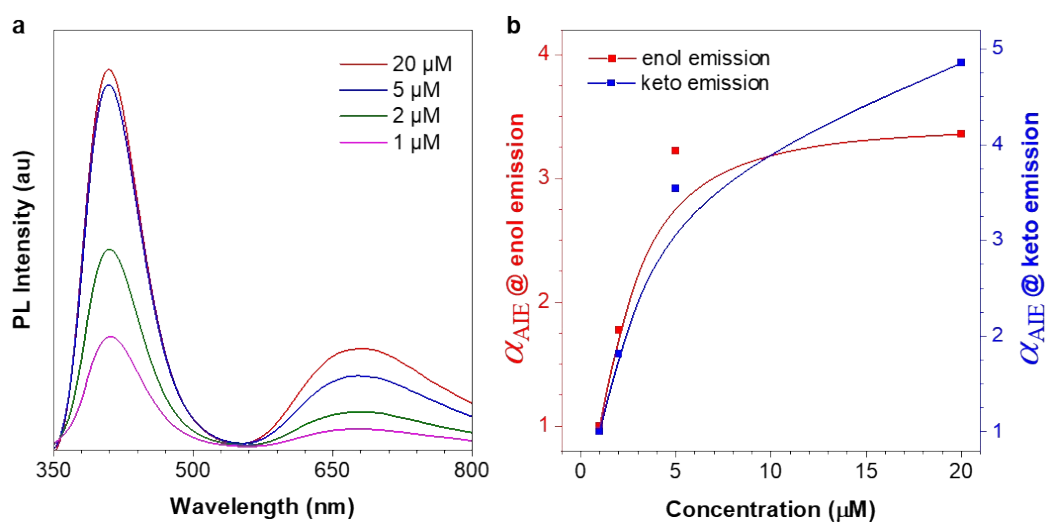


Figure S11. PL spectra of *o*-Br-TPA in ACN solution with different concentrations. $\lambda_{\text{ex}} = 326$ nm.

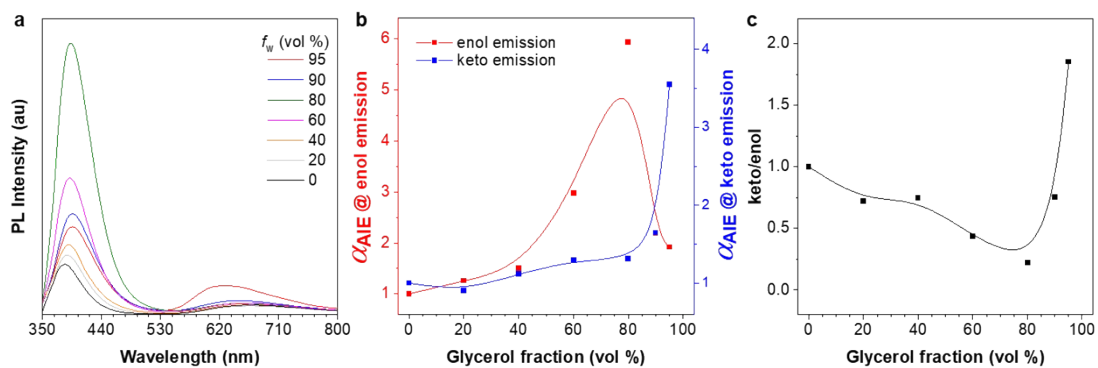


Figure S12. (a) PL spectra of *o*-Br-TPA in EtOH/glycerol mixtures with different fractions of glycerol. (b) The plots of the enol and keto emission intensity at the maximum versus the composition of the glycerol mixture of *o*-Br-TPA. $\alpha_{\text{AIE}} = I/I_0$, I_0 = PL intensity in pure EtOH. (c) The plot of keto/enol emission intensity at the maximum versus the composition of the glycerol mixture of *o*-Br-TPA. Concentration: 20 μM . λ_{ex} : 326 nm.

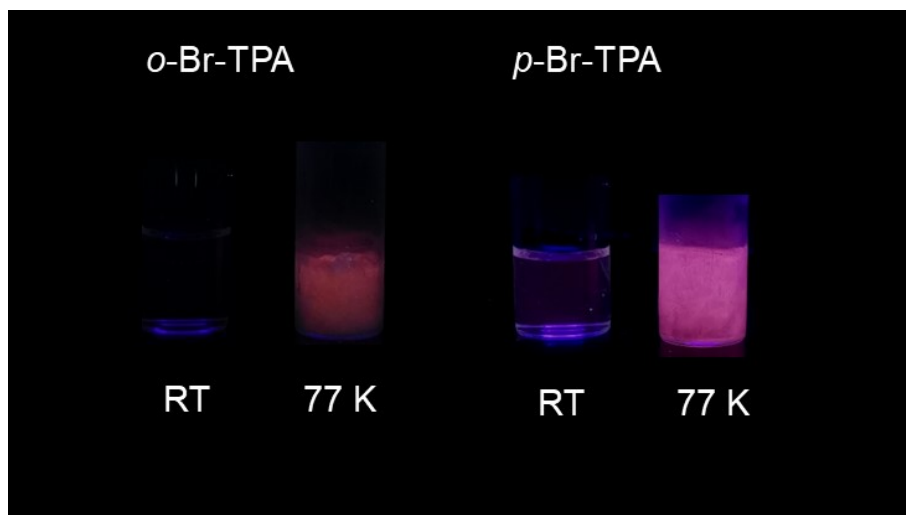


Figure S13. Fluorescence photographs of *o*-Br-TPA (in ACN), and *p*-Br-TPA (in THF) at RT and 77 K, respectively. λ_{ex} : 365 nm. Concentration: 20 μM .

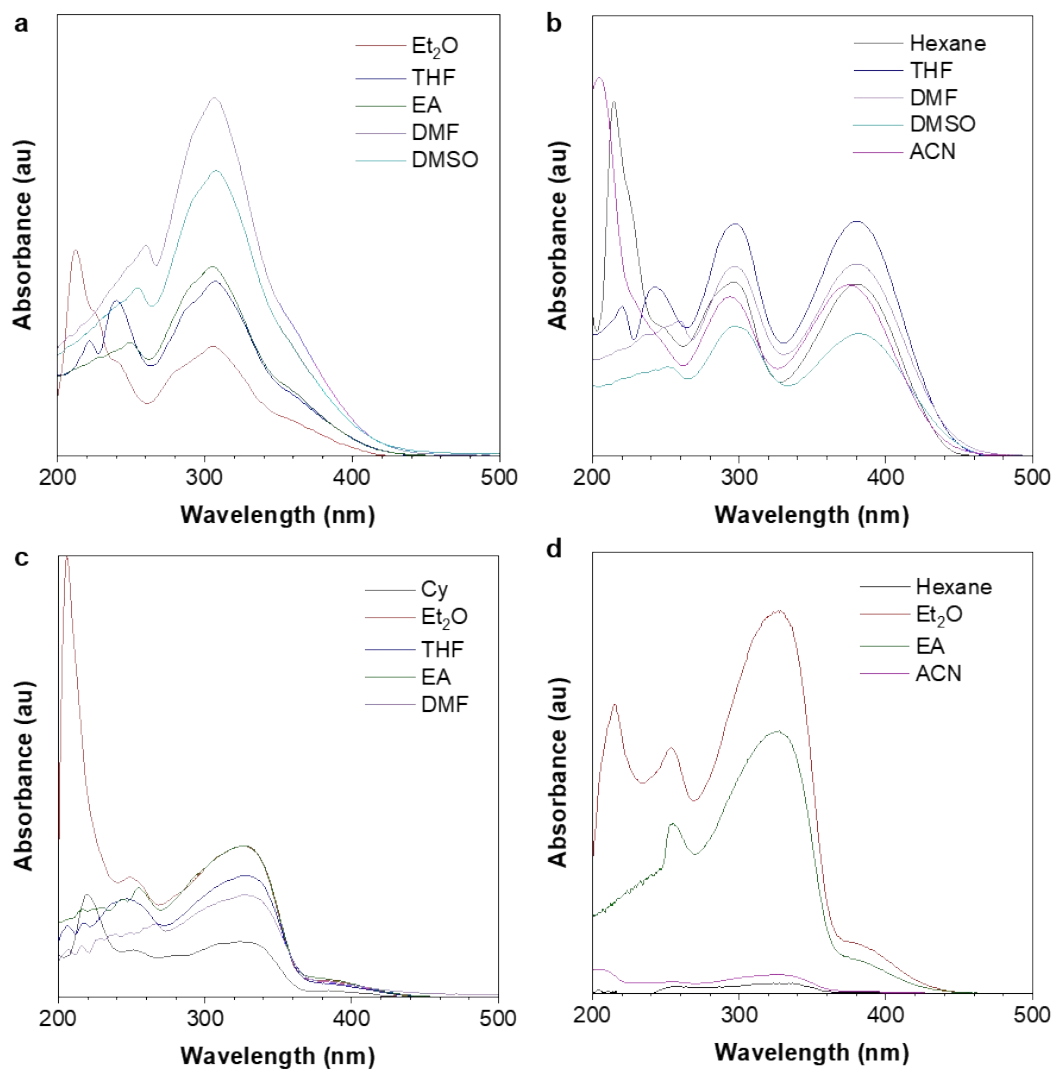


Figure S14. Absorption spectra of (a) *o*-TPA-Br, (b) *p*-TPA-Br, (c) *o*-Br-TPA, and (d) *p*-Br-TPA in solvents of varying polarity. Concentration: 20 μ M.

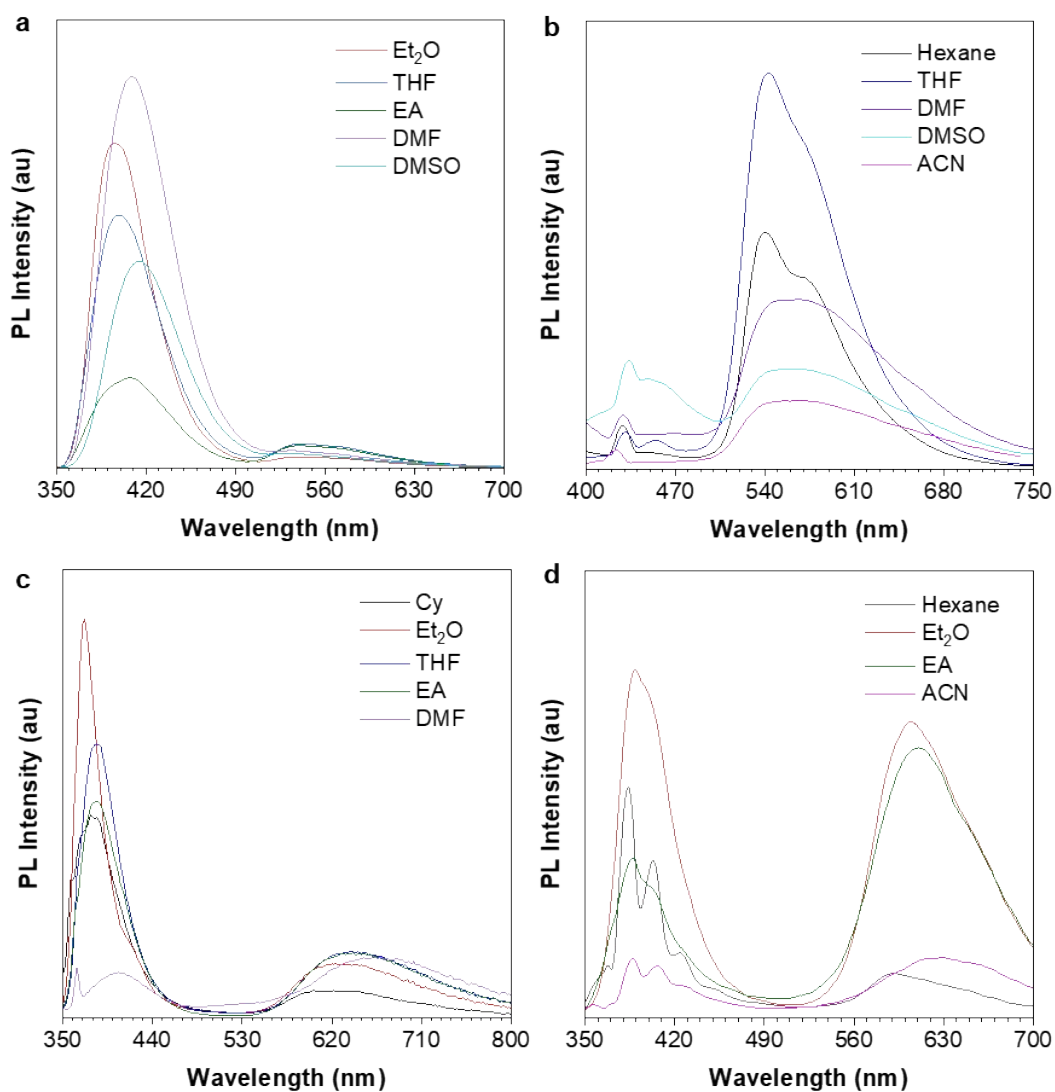


Figure S15. The PL spectra of (a) *o*-TPA-Br, (b) *p*-TPA-Br, (c) *o*-Br-TPA, and (d) *p*-Br-TPA in solvents of varying polarity. Concentration: 20 μ M.

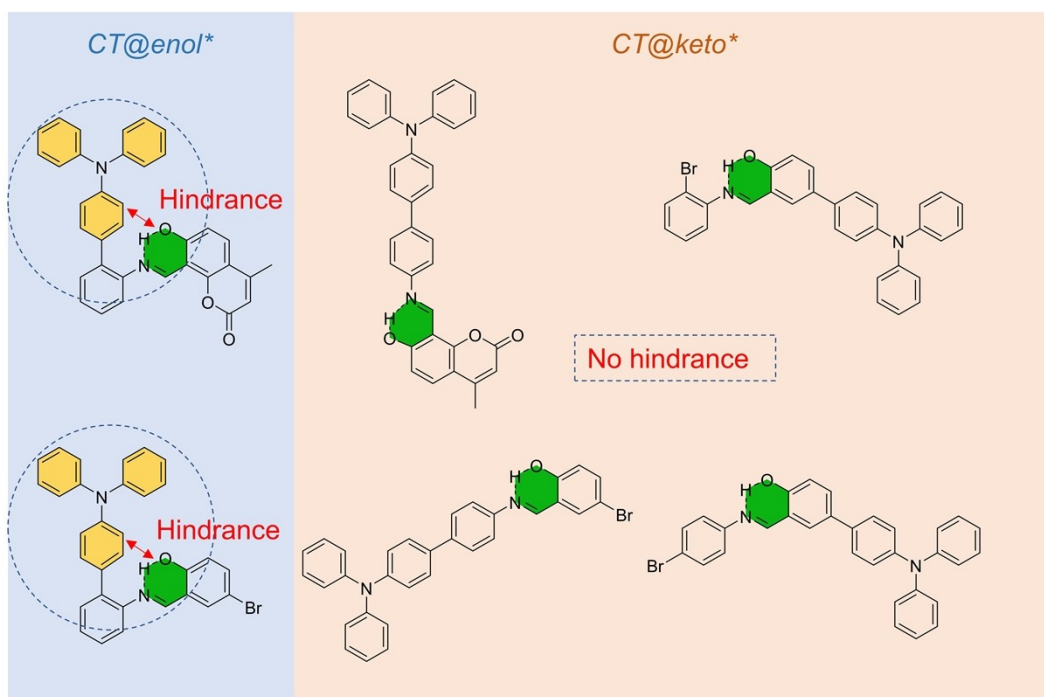


Figure S16. The molecular structures of isomers that regulate excited-state processes.

Table S1. Crystallographic data for *o*-Br-TPA and *p*-Br-TPA.

| | <i>o</i> -Br-TPA | <i>p</i> -Br-TPA |
|---|--|--|
| empirical formula | C ₃₁ H ₂₃ BrN ₂ O | C ₃₁ H ₂₃ BrN ₂ O |
| <i>M_r</i> | 519.42 | 519.42 |
| cryst syst | monoclinic | monoclinic |
| space group | P21/c | I2/a |
| <i>a</i> (Å) | 19.02(3) | 15.4196(10) |
| <i>b</i> (Å) | 13.300(18) | 7.0728(5) |
| <i>c</i> (Å) | 9.799(14) | 44.912(2) |
| <i>α</i> (°) | 90 | 90 |
| <i>β</i> (°) | 100.93(3) | 93.069(5) |
| <i>γ</i> (°) | 90 | 90 |
| <i>V</i> (Å ³) | 2434(6) | 4891.1(5) |
| <i>Z</i> | 4 | 8 |
| <i>ρ_c</i> (g cm ⁻³) | 1.418 | 1.411 |
| <i>F</i> (000) | 1064.0 | 2128.0 |
| <i>T</i> (K) | 296.15 | 293(2) |
| <i>μ</i> (mm ⁻¹) | 1.716 | 2.495 |
| data / restraints / parameters | 4284/0/317 | 4699/0/317 |
| GOF (<i>F</i> ²) | 1.065 | 1.065 |
| <i>R</i> ₁ ^a , <i>wR</i> ₂ ^b (<i>I</i> > 2σ(<i>I</i>)) | 0.0952, 0.1768 | 0.0780, 0.1931 |
| <i>R</i> _{int} | 0.1181 | 0.0598 |

^a $R_1 = \Sigma(|F_o| - |F_c|) / \Sigma|F_o|$; ^b $wR_2 = \{\Sigma[w(F_o^2 - F_c^2)^2] / \Sigma[w(F_o^2)^2]\}^{1/2}$

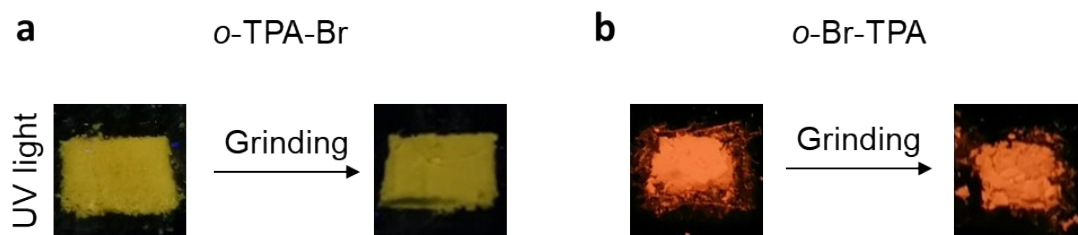


Figure S17. The photographs of (a) *o*-TPA-Br and (b) *o*-Br-TPA before and after grinding tanken under 365 nm lamp irradiation.

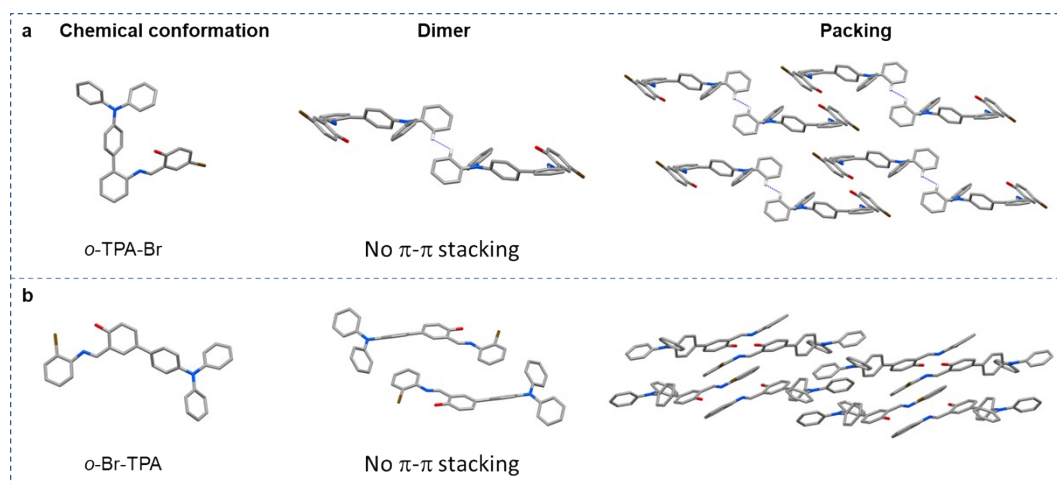


Figure S18. The chemical conformations, dimers, and packings of (a) *o*-TPA-Br and (b) *o*-Br-TPA.

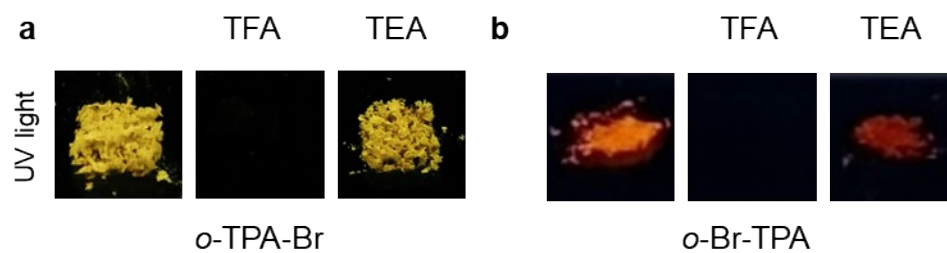


Figure S19. Fluorescence photographs of (a) *o*-TPA-Br and (b) *o*-Br-TPA as solid (pristine, sample fumed with TFA, sample fumed with TEA).

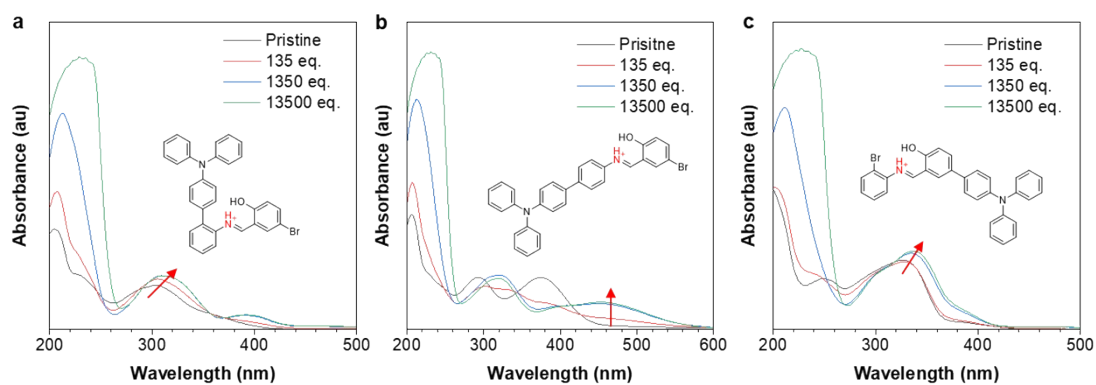


Figure S20. Absorption spectra of (a) *o*-TPA-Br, (b) *p*-TPA-Br, and (c) *o*-Br-TPA in pure ACN by adding different equivalents of TFA. Concentration: 20 μ M.

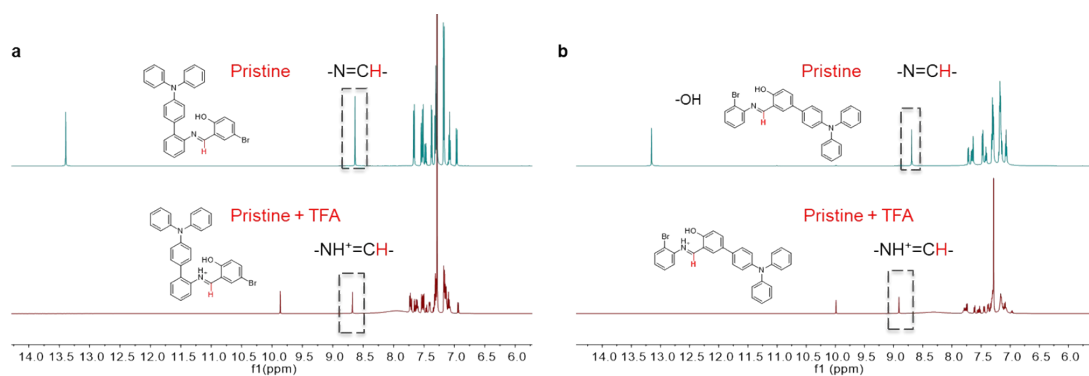


Figure S21. ^1H NMR spectra of (a) *o*-TPA-Br and (b) *o*-Br-TPA in CDCl_3 before and after TFA fuming in 6.0–14.0 ppm region.



Figure S22. Fluorescence photographs of the ground *p*-TPA-Br before and after TFA/TEA treatments.

References

- [1] X.-M. Cai, W. Zhong, Z. Deng, Y. Lin, Z. Tang, X. Zhang, J. Zhang, W. Wang, S. Huang, Z. Zhao, and B. Z. Tang, *Chem. Eng. J.*, 2023, **466**, 143353.